

**Supplemental Figure 1. Sequences for the primers used in ChIP and q-RTPCR analyses.**

**Supplemental Figure 2. FXR binds to key component genes of the FGF19 signaling pathway.** Browser images from liver ChIP-seq data from mice treated with GW4064 for 1 h (Lee et al., Hepatology, 2012) using the UCSC genome browser. The direction of gene transcription is indicated by the arrow and the beginning of the arrow indicates the position of the transcriptional start site (TSS).

**Supplemental Figure 3. Effects of pharmacological activation of FXR on *βKL* and *Fgfr4* mRNA levels.** Hepatocytes were isolated from WT or FXR-KO mice, were treated with 500 nM GW4064, and then, *βKL* and *Fgfr4* mRNA levels were measured by q-RTPCR. SEM, n=6.

**Supplemental Figure 4. Potential FXR binding sites as detected by the nuclear receptor binding motif search engine NUBIScan in the 700 bp genomic fragment of *βKL* containing a FXR binding site identified in ChIP-seq studies.**

**Supplemental Figure 5. Adenoviral-mediated FXR compensation experiments in FXR-KO mice.** C57BL/6 wild-type (WT) and FXR knockout (FXR-KO) mice were tail-vein injected with either control Ad-Empty or Ad-FXR. One week later, livers were collected, and mRNA levels of *βKL* and *Fgfr4* were measured by q-RTPCR.

**Supplemental Figure 6. Effects of GW4064 treatment for different times on hepatic *βKL* protein levels.** WT mice were injected with GW4064 for the times indicated. *βKL* protein levels in the liver were detected by IHC. Representative images of hepatic *βKL* from 3 independent IHC studies are shown.

**Supplemental Figure 7. Pre-treatment with GW4064 enhances responsiveness to FGF19 signaling in primary human hepatocytes.** Primary human hepatocytes (PHH) were pre-treated with GW4064 for 2 h, and then treated with FGF19 for 30 min. Protein levels of total (T-Erk) and phosphorylated (P-Erk) ERK were measured by IB (shown in duplicate).

## Supplemental Figures

Sequences for the primers used in ChIP and q-RT-PCR analyses.

Chip qPCR primers	
Grb2 qChip-f1	AAGAGCACCCGTGCAAATAC
Grb2 qChip-r1	GAAGGATTTTCCCCATGT
Sos2 qChip-f1	ATGAGTCTTTGGGCAAGAGG
Sos2 qChip-r1	TCACAGTAGACAGGCCAGAATG
Ras qChip-f1	TTCACGACACAAAGCCACTC
Ras qChip-r1	AGGAGGTGGAGGTAGGGATG
Raf qChip-f1	CCGGGTCTTTGTGAAGTAG
Raf qChip-r1	TGTGTTGCTGGGACTTGAAC
Map2k1 (Mek1) qChip-f1	GACATGTTTCAGAGGCAGCA
Map2k1 (Mek1) qChip-r1	TAGGTTTCAGCAGGCAGAGG
Ppp2cb qChip-f1	TCCTGTCTTCTCCACCTG
Ppp2cb qChip-r1	GATACTCCACCCAGCAGA
Map2k6 (Mek6) qChip-f1	TGCTAGGTGCCTTCCTGTCT
Map2k6 (Mek6) qChip-r1	GCTCAGTGGGTGGAGTGTTC
Mapk3 (Erk1) qChip-f1	TGAGGCAGGTCTTCAAAGGT
Mapk3 (Erk1) qChip-r1	CGCCTAGTTACGCTGTTCT
βKL qChip-f1	GGCTCTGCAAAAAGGAACAG
βKL qChip-r1	CAGGTAACCCCTTGTCCA

Cloning /EMSA primers	
βKL(700bp-wt)-Luc-f1	TTACTCGAGTATCATGCGCTGAGACATGAACT
βKL(700bp-wt)-Luc-r1	TAGAGATCTCTAGCTGCGTTCTAAGCTGTTCC
βKL(552bp-wt)-Luc-f1	TTGGTACCTACCCAGCACCCGAATAAAAC
βKL(552bp-wt)-Luc-r1	TTGCTAGCCATCTCGTGGTCTGGTTTCCC
βKL(195bp)-Luc-f1	TTGGTACCTAGAGTTTGACCCAGCAC
βKL(195bp)-Luc-r1	TGCTAGCCTAGTGATGCCTCTGTGTGGATG
βKL(700bp-mut)-Luc-f1	TATATACAGGCCCTTTAATTACATATATTTCACTTGGAC
βKL(700bp-mut)-Luc-r1	GTCCAAGTGAAATATATGTAATTAAGGGCCTGTATATA
βKL IR2 EMSA-f1	CAGGCCCTTGGGTCAAATGTCTTTCACTTGGAC
βKL IR2 EMSA-r1	GTCCAAGTGAAAGACATTTGACCCAAGGGCCTG
Shp IR1 EMSA-f1	TGGTACAGCCTGAGTTAATGACCTTGTATC
Shp IR1 EMSA-r1	GATAACAAGGTCATTAACCTCAGGCTGTACCA

**Sequences for the primers used in ChIP and q-RT-PCR analyses. (Con't)**

qPCR primers	
m36B4-F	CGACATCACAGAGCAGGC
m36B4-R	CACCGAGGCAACAGTTGG
mβKL-F	CGAGCCATTGTTACCTTGT
mβKL-R	CTCCAAAGGTCTGGAAGCAG
mFgfr4-F	GACCAAACCAGCACCGTGGCTGTGAAGATG
mFgfr4-R	GTTCCCTTGGCGGCACATTCCACAATCA C
mGrb2-F	TCAATGGGAAAGATGGCTTC
mGrb2-R	GAGCATTCTTCTGCCTTGG
mSos2-F	TGTTCTGCATCAAATCCAA
mSos2-R	AGATGCTGTGCTTCCGTCT
mRas-F	GGCTGTGCTGGAGACTAAG
mRas-R	CTTCTGGCTCACCTGCCTAC
mRaf-F	TTCAGTGGCTGTAGTCTGG
mRaf-R	ACTGTCCACTTCCCCTTCT
mMek1-F	CTAGTGACCTGGGTGGTCTGT
mMek1-R	CACAAGGCTCCCTCTCAGAC
mPpp2cb-F	GGGGTCTGGTCACTTGAAAA
mPpp2cb-R	GATACTTCCACCCAGCAGA
mMek6-F	ACTGGTCGACCTACTGTGG
mMek6-R	CCCCTTGGAGAGGAAAAAG
mErk1-F	TCCTTTGGATCTGGTCTG
mErk1-R	CCCAGCAAAGTGAGAGAAG
mCyp7a1-F	CATCTCAAGCAAACACCATTC
mCyp7a1-R	TCACTTCTCAGAGGCTGGTTTC
mCyp8b1-F	GAACCAACAGGCCATGCT
mCyp8b1-R	AGGAGCTGGCACCTAGACT
mShp-F	CAAGAAGATTCTGCTGGAGG
mShp-R	GGATGTCAACATCTCCAATG
h36b4-F	GGTCCTCCTTGGTGAACAC
h36b4-R	AAGGCTGTGGTCTGATG
hCyp7a1-F	CAAGGAATCGCTGAGGCTTTC
hCyp7a1-R	ACCGTCTCAAGGTGCAAAGT
hCyp8b1-F	AAGCATGGGGATGTGTTAC
hCyp8b1-R	CAAACCTGCGGAACTCCATG
mFgf15 premRNA-F	CATGCACACGCCTCTTGTG
mFgf15 premRNA-R	TCCATTTCTCCTGAAAGGT
mβKL premRNA-F	TCGCTGCTTCTTTTCTCTG
mβKL premRNA-R	ATAGGCATCCTGCCACTCAA
mFgfr4 premRNA-F	CCTCTCCTTGTCTGGCTTT
mFgfr4 premRNA-R	CACCTTCCATCACAGGCTC
mSHP premRNA-F	CAACTATCCGAAGGCCACAT
mSHP premRNA-R	ACCCTCTCTACCCACCCACT
mcyp7a1 premRNA-F	TTTGATCATGGCTTCAAG
mcyp7a1 premRNA-R	TCTTCCAGACACTCCCAAC

**Fig. S1. Sequences for the primers used in ChIP and q-RT-PCR analyses.**

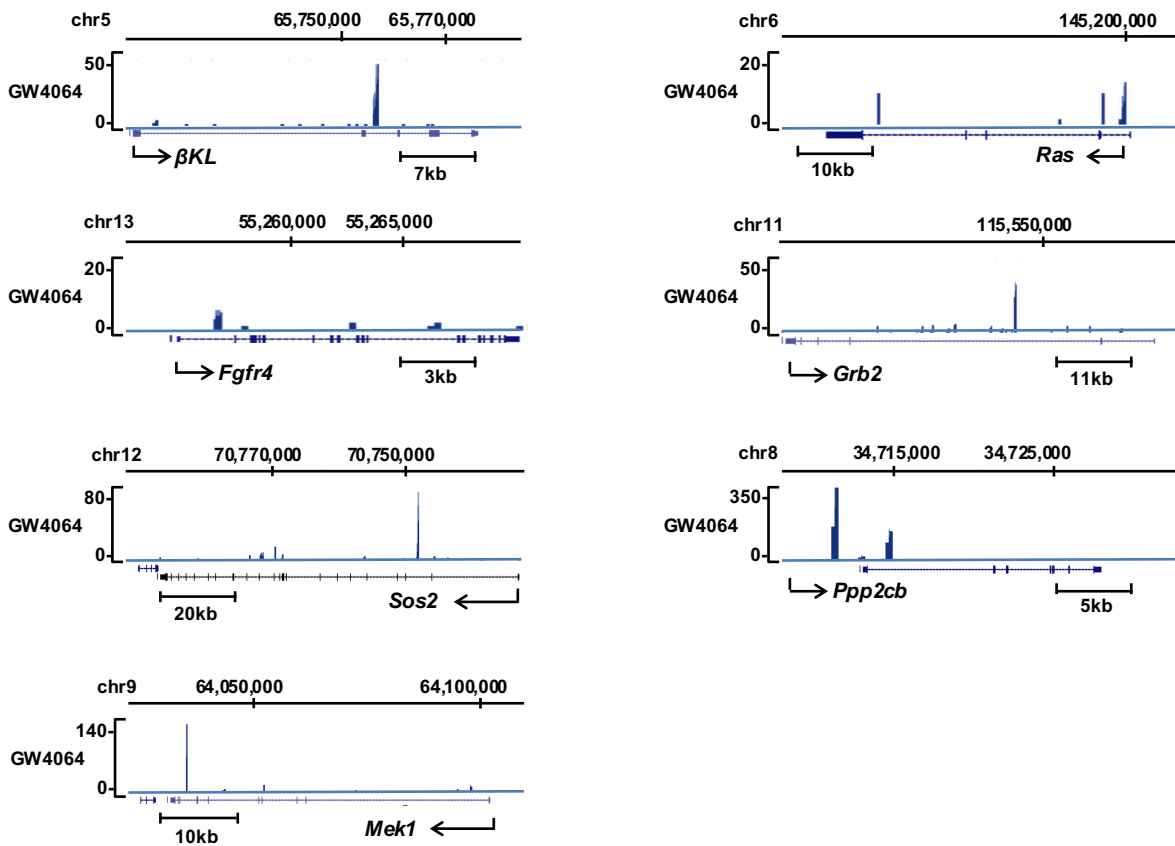


**Fig. S2. FXR binds to key component genes of the FGF19 signaling pathway.** Browser images from liver ChIP-seq data from mice treated with GW4064 for 1 h (Lee et al., Hepatology, 2012) using the UCSC genome browser. The direction of gene transcription is indicated by the arrow and the beginning of the arrow indicates the position of the transcriptional start site (TSS).

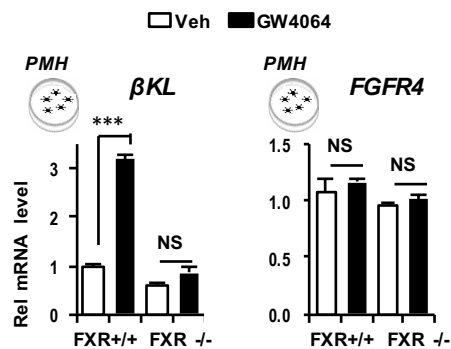


**Fig. S3. Effects of pharmacological activation of FXR on  $\beta$ KL and Fgfr4 mRNA levels.** Hepatocytes were isolated from WT or FXR-KO mice, were treated with 500 nM GW4064, and then,  $\beta$ KL and Fgfr4 mRNA levels were measured by q-RT-PCR. SEM, n=6.

Graphical representation of the predictions along your sequence.

**X axis:** position in basepairs

**Y axis:** raw score on sense (top) and antisense (bottom) strand

**FXR binding peak region, 700bp**  
(chr5:65,764,431–65,765,130)

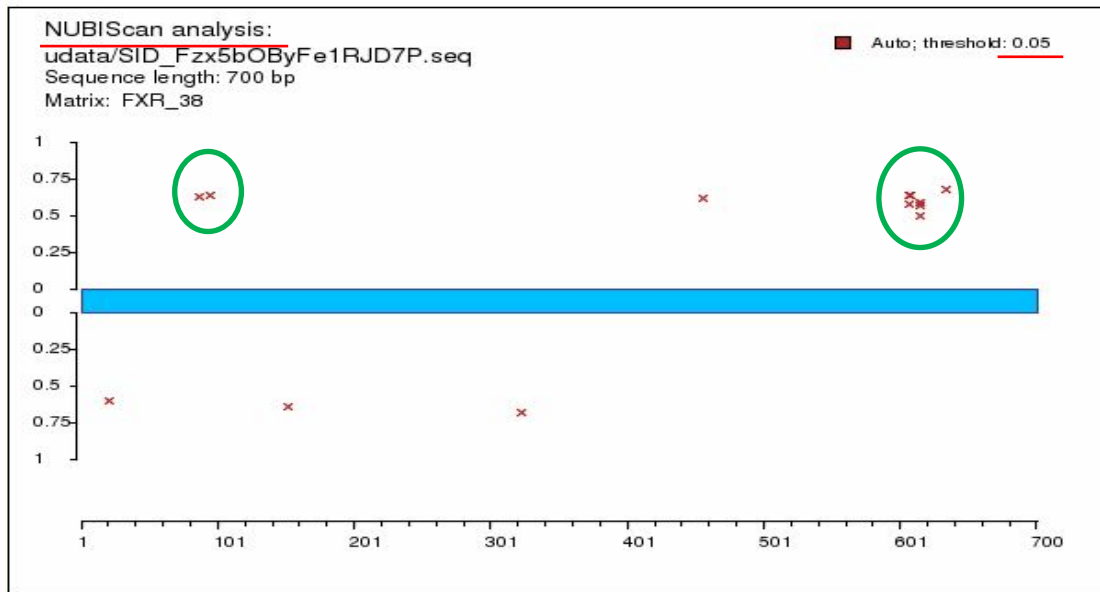


**Fig. S4. Potential FXR binding sites as detected by the nuclear receptor binding motif search engine NUBIScan in the 700 bp genomic fragment of  $\beta$ KL containing a FXR binding site identified in ChIP-seq studies.**

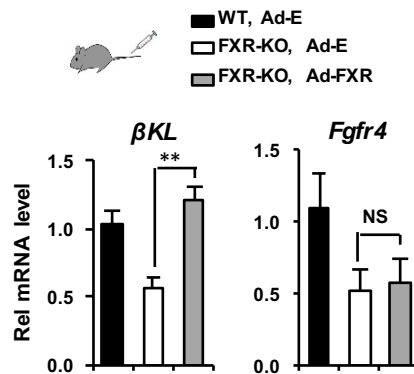


**Fig. S5. Adenoviral-mediated FXR compensation experiments in FXR-KO mice.** C57BL/6 wild-type (WT) and FXR knockout (FXR-KO) mice were tail-vein injected with either control Ad-Empty or Ad-FXR. One week later, livers were collected, and mRNA levels of  $\beta$ KL and Fgfr4 were measured by q-RT-PCR.

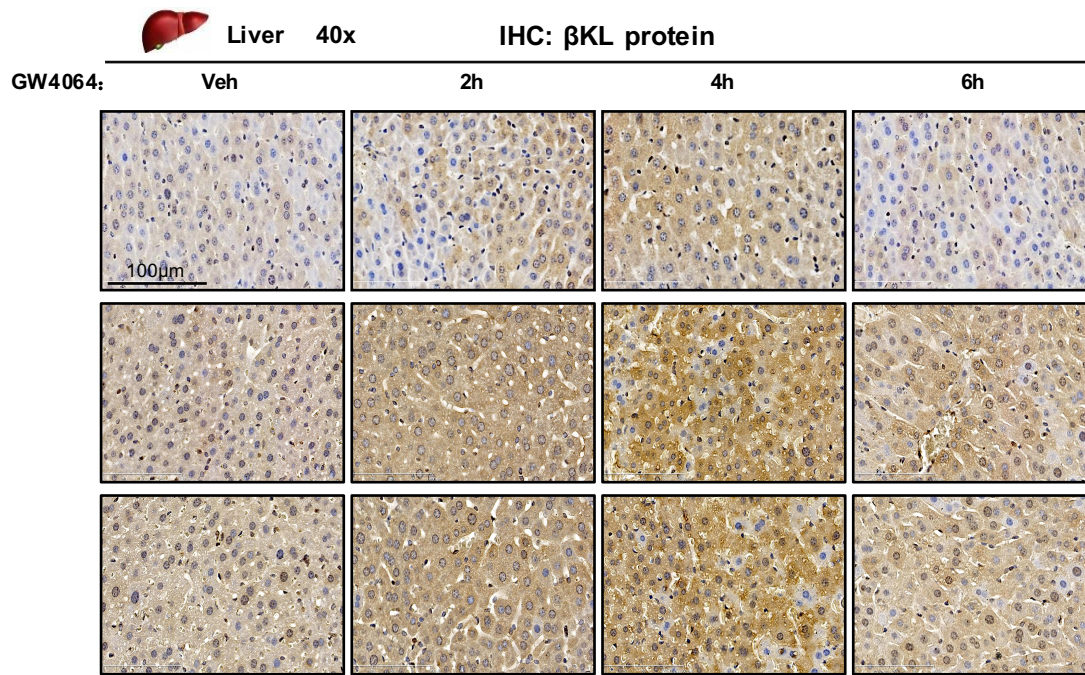


**Fig. S6. Effects of GW4064 treatment for different times on hepatic  $\beta$ KL protein levels.** WT mice were injected with GW4064 for the times indicated.  $\beta$ KL protein levels in the liver were detected by IHC. Representative images of hepatic  $\beta$ KL from 3 independent IHC studies are shown.

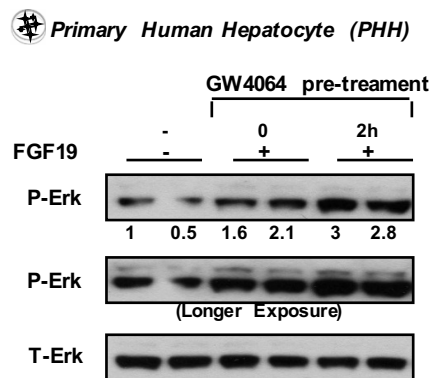


**Fig. S7. Pre-treatment with GW4064 enhances responsiveness to FGF19 signaling in primary human hepatocytes.** Primary human hepatocytes (PHH) were pre-treated with GW4064 for 2 h, and then treated with FGF19 for 30 min. Protein levels of total (T-Erk) and phosphorylated (P-Erk) ERK were measured by IB (shown in duplicate).